Journal of Catalysis **188,** 237–251 (1999)
Article ID jcat.1999.2661, available online at http://www.idealibrary.com on IDEAL®

Heat of Adsorption of Carbon Monoxide on a Pd/Al_2O_3 Solid Using *in Situ* Infrared Spectroscopy at High Temperatures

Olivier Dulaurent,* Karine Chandes,† Christophe Bouly,† and Daniel Bianchi*,[1]

*Laboratoire d'Application de la Chimie à l'Environnement (LACE), UMR 5634, Université Claude Bernard, Lyon-I,
Bat. 308, 43 Bd du 11 Novembre 1918, 69622 Villeurbanne, France; and †ECIA—Equipement et Composants
pour l'Industrie Automobile, BP 17-Bois sur prés, 25 550 Bavans, France

Received December 15, 1998; revised August 5, 1999; accepted August 6, 1999

The adsorption of CO (1% CO/He mixture, 1 atm total pressure) on a reduced 1.4% Pd/Al_2O_3 solid is studied in the temperature range 300–800 K by in *situ* Fourier transform infrared (FTIR) spectroscopy using a suitably constructed small-internal-volume infrared cell. Two main IR bands are detected above and below 2000 cm^{-1}, ascribed to linear and bridged adsorbed CO species on palladium atoms, respectively. The change in IR band intensities with adsorption temperature is used to determine the evolution in the coverage θ of the various adsorbed species with this parameter. The observed curves are in good accord with an adsorption model assuming a linear decrease in the heats of adsorption in step with the increase in coverage. This allows determination of the heats of adsorption of each species at various coverages. For instance, at $\theta \approx 0$, the heats of adsorption are 92 and 168 kJ/mol for the linear and bridged CO species, respectively. These values decrease respectively to 54 and 92 kJ/mol at $\theta \approx 1$. As previously observed on platinum-containing solids, the disproportionation reaction $2CO \rightarrow C_{ads} + CO_2$ detected at high temperatures (a) limits the adsorption temperature and the partial pressures of CO, and (b) creates some changes in the surface of the palladium particles. The heats of adsorption of the adsorbed species determined according to the present experimental procedure are discussed in relation to data in the literature concerning various Pd-containing solids: monocrystals, model particles, and supported catalysts. Several experimental data, i.e., effects of aging of the solid, are presented and discussed in relation to the heats of adsorption of CO.

I. INTRODUCTION

Characterization of the adsorption of carbon monoxide on metal-supported catalysts is the subject of numerous catalysis studies in relation to the catalytic reactions involving this compound (i.e., CO/H_2, CO/O_2, CO/NO). Fourier transform infrared (FTIR) spectroscopy has been extensively used in this field because it enables characterization of the chemical structure of the adsorbed CO (i.e., linear, bridged, *gem*-dicarbonyl), as well as the oxidation state of the sites. For instance, with palladium catalysts, FTIR leads to the identification of the linear CO species adsorbed either on $Pd^{+\delta}$ or on Pd^0 (1, 2). Another parameter studied to characterize CO chemisorption is the heat of adsorption on the metallic part of the catalysts. For instance, in the case of palladium, the studies realized on monocrystals have shown that CO is adsorbed mainly in the form of bridged species (3–5) and that the heats of adsorption, at low coverages, change but not significantly with the exposed plane in the range 140 kJ/mol for Pd (111) to 170 kJ/mol for Pd (110) (6–9). It is observed that the heat of adsorption decreases with increase in coverage (6, 10, 11) whatever the exposed plane. After the adsorption of CO at room temperature on supported palladium particles, FTIR spectroscopy shows that, in addition to the IR bands of the bridged species (more than one bridged species can be detected), an IR band appears at ≈2080 cm^{-1} and is attributed to a linear CO species, as observed on various metallic oxides (12–19 and references therein): Al_2O_3 (12, 13), SiO_2 (14–16), TiO_2 (17), MgO (18), and La_2O_3 (19). The proportion of linear CO species relative to the bridged CO species is a function of various parameters such as metal dispersion. For instance, on Pd/SiO_2 catalysts, the ratio intensity of the IR band of the bridged CO species/intensity of the IR band of the linear CO species decreases with decrease in particle size, from about 10 for a dispersion of 0.1 to 2 for a dispersion of 1 (14). The heats of adsorption of the adsorbed CO species can be obtained using temperature-programmed desorption (TPD) measurements, given that the adsorption is not activated. However, for metal-supported catalysts, the experimental data can be influenced by various parameters such as diffusion and readsorption which may affect the value of the activation energy of the desorption (20, 21). These difficulties explain the interest shown in the microcalorimetric measurements to determine the heats of adsorption of CO on metal-supported catalysts, in particular Pd (9, 22). It has been noted (9) that the heat of adsorption of CO: (a) is not noticeably affected by the nature

---

[1] To whom correspondence should be addressed. E-mail: daniel.bianchi@univ-lyon1.fr.

0021-9517/99 $30.00

of the support (SiO_2, Al_2O_3, SiO_2/Al_2O_3, and TiO_2); (b) is constant over a large range of particle sizes (1000–3 nm); and (c) increases sharply for particles smaller than 3 nm (9). Taking into account the formation of at least two adsorbed CO species (linear and bridged) on reduced palladium-supported catalysts, the microcalorimetric experiments can be considered to provide an average of the heats of adsorption of the various species and the evolution of their proportions with dispersion (14) can be considered to influence the experimental values.

Better characterization of the adsorption of CO on supported Pd catalysts imposes the determination of the contribution of each adsorbed species to the heat of adsorption of CO. In a previous study (23), on platinum-containing solids (in particular a three-way catalyst), we showed that studying the change in the intensity of the IR band of the linear CO species relative to the adsorption temperature can lead to the determination of the heat of adsorption of this adsorbed species at various coverages θ. On platinum-supported catalysts, the bridged CO species usually gives a weak IR band below 2000 cm^{-1} and good accord was observed with the microcalorimetric measurements (23). In particular we have observed that the heat of adsorption of the linear CO species decreases with increase in coverage according to a linear relationship for $\theta > 0.36$.

In the present study, the procedure developed previously (23) is used to measure the heat of adsorption of each adsorbed CO species (linear and bridged) on a 1.4% Pd/Al_2O_3 solid. The results are compared with data in the literature on Pd-containing solids: monocrystals, model particles, and supported catalysts. We have particularly taken account of studies performed under experimental conditions similar to those of the present study (adsorption equilibrium conditions) (10, 11, 24). Some other experimental data are presented and discussed in relationship to the heats of adsorption of the adsorbed CO species such as aging of the solid (particle size effect) and isothermal desorption at room temperature.

II. EXPERIMENTAL

a. Catalyst

The 1.4% Pd/Al_2O_3 (in wt%) solid is prepared according to the following procedure: γ-alumina (100 m^2/g) from Condea is introduced slowly into an aqueous solution of $Pd(NH_3)_4(NO_3)_2$ (the final solution/alumina weight ratio is around 4). After 24 h agitation at room temperature, the suspension is heated slowly to evaporate the solvent. The powder obtained is treated in air for 4 h at 393 K followed by 2 h at 773 K. The BET area of the solid is 95 m^2/g.

For the FTIR studies, the powder is compressed to form a disk ($\Phi = 1.8$ cm, weight range 38–90 mg) which is placed in the sample holder of the IR cell described below.

Before the adsorption of CO (using a 1% CO/He mixture), the solid is treated *in situ* (150 cm^3/min) according to the following procedure: oxygen ($T = 713$ K, $t = 30$ min) $\rightarrow$ helium ($T = 713$ K, $t = 30$ min) $\rightarrow$ hydrogen ($T = 713$ K, $t = 30$ min.) $\rightarrow$ hydrogen (adsorption temperature) $\rightarrow$ helium (10 min) $\rightarrow$ 1% CO/He. It is well known that CO displaces the adsorbed hydrogen on Pd-containing solids (13 and references therein). Some results, however, are also presented on the solid treated for 10 min in He at 713 K after the reduction step, before cooling down to room temperature in He. The amount of CO adsorbed at room temperature on the reduced Pd/Al_2O_3 catalyst using the experimental method described in (23) is 32 μmol/g of catalyst.

b. High-Temperature IR Cell for Transient Experiments

FTIR spectra of the adsorbed CO species on the prepared solids, in presence of the CO/He mixture, are recorded by using a small-internal-volume stainless-steel IR cell described elsewhere (23). The solid, compressed to form a disk, is placed between two CaF_2 windows 2.2 mm apart. This small volume increases the ratio between the incoming signal due to the adsorbed species and the signal due to the gas-phase species. This cell enables *in situ* treatments (293–900 K) of the solid, at atmospheric pressure, with a gas flow rate in the range 150–2000 cm^3/min.

III. RESULTS AND DISCUSSION

The main objective of the present study is the determination of the heats of adsorption of the linear and the bridged CO species adsorbed on reduced palladium particles of 1.4% Pd/Al_2O_3 solid under adsorption equilibrium conditions. We, however, observed a change in the Pd surface during the first experiments (adsorption of CO at various temperatures followed by pretreatment of the solid at 713 K), leading to the decrease in the intensities of the IR bands observed after adsorption of CO at room temperature. The experiments initially described were performed on a catalyst pellet which has been submitted to at least the two following cycles: initial pretreatment (see above) $\rightarrow$ 1% CO/He, 293 K $\rightarrow$ 1% CO/He, 740 K $\rightarrow$ pretreatment. The modifications of the catalyst during the first experiment and their effects on the observed IR spectra are presented in the final part of this study.

a. Adsorption of CO on Reduced Pd/Al_2O_3 Catalyst

Figure 1 shows the FTIR spectrum at 300 K after introduction of the 1% CO/He mixture on the reduced Pd/Al_2O_3 catalyst (spectrum a). This spectrum is similar to those observed in various studies on palladium-supported particles (14–16, 19, 25, 26). The IR band observed at 2072 cm^{-1} is attributed, according to the literature, to a linear CO species

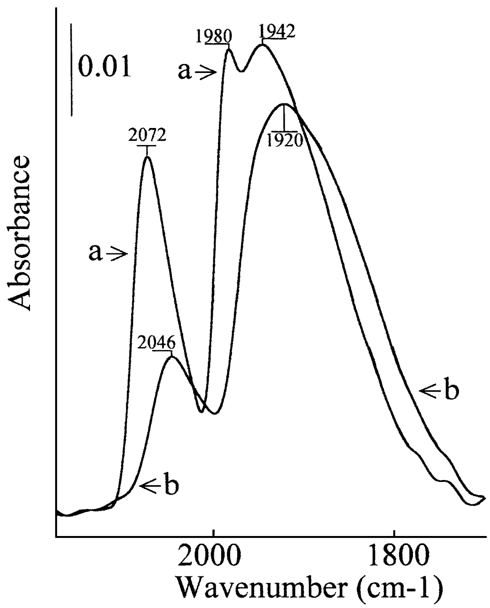

FIG. 1. Adsorption of CO (1% CO/He) on the reduced 1.4% Pd/Al_2O_3 solid at two temperatures: (a) 300 K and (b) 568 K.

on the palladium atoms (species noted as L). Note that in the cited literature, the IR band of the linear species is located at 2080 ± 10 cm^{-1}, with a larger number of studies indicating a position at ≈2085 cm^{-1}. This remark is discussed in the final part of the present study in relation to high-temperature helium treatment of the solid after the reduction. The sites that lead to the L species are mainly considered to be low-coordinated (edges, corners, etc.) palladium atoms (14–16). The linear adsorbed species, however, is also detected on Pd (100) (27) and Pd (111) (10), and some authors (15, 19, 28) believe that on supported catalysts, the sites may be situated in the middle of the crystal planes. This shows that it cannot be excluded that the IR band detected around 2080 cm^{-1} on Pd-supported catalysts can be attributed to two types of linear CO species as considered in (15). In Fig. 1 (spectrum a) the IR bands detected at 1980 and 1942 cm^{-1} can be attributed to two bridged CO species corresponding to sites situated on different Pd planes. The two species are referenced B_1 (1980 cm^{-1}) and B_2 (1942 cm^{-1}), respectively, according to the literature. The sites adsorbing the B_1 and B_2 species are assessed as being situated on Pd (100) or on Pd (110) and on Pd (111), respectively (15–17, 19). Note that the B_2 species is often detected in the form of a shoulder on the IR band of the B_1 species (12, 14–16, 26) but the reverse is also reported (13). Spectrum b in Fig. 1 was recorded at 568 K in presence of the 1% CO/He mixture after heating from 300 K at 5 K/min. The IR band of the L species shifts to a lower wavenumber (2046 cm^{-1}) and its intensity decreases. At 568 K, the IR band of the B_1 species is no longer detected and the IR band of the B_2 species shifts to 1920 cm^{-1} while its intensity decreases. In the following section, the progressive decrease in the intensities of the IR bands of each adsorbed species with the increase in adsorption temperature is used to determine their heats of adsorption at various coverages. To facilitate the presentation, the results related to the L species are described first, even if the L and B species are studied in the course of the same experiments.

b. Change in Coverage of Linear CO Species with Adsorption Temperature

Figure 2 shows the FTIR spectra, in the range 2200–2000 cm^{-1}, recorded at several adsorption temperatures on the pretreated Pd/Al_2O_3 solid. Introduction of the 1% CO/He mixture (100 cm^3/min) at 300 K on the reduced solid leads to the appearance of a high-intensity IR band at 2072 cm^{-1} (spectrum a, Fig. 2). Initially, the increase in adsorption temperature (≈5 K/min) does not change the intensity of the IR band up to 328 K (spectrum b). At higher temperatures, the intensity decreases progressively alongside a shift of the IR band to lower wavenumbers (i.e., 2065 cm^{-1} at 368 K, 2053 cm^{-1} at 468 K, and 2045 cm^{-1} at 578 K) according to a linear relationship in a large range of temperatures (328–578 K). At temperatures higher than 578 K, the position of the IR band is constant. Note that the IR band is still detected at 723 K. Figure 3 compares the FTIR spectra recorded at room temperature before (spectrum a) and after (spectrum b) heating in CO at 723 K. It is observed that the treatment in CO does not significantly modify the intensity of the IR band but leads to a shift to a higher wavenumber (2088 cm^{-1}). This indicates that carbon deposition, at high temperatures, due to the

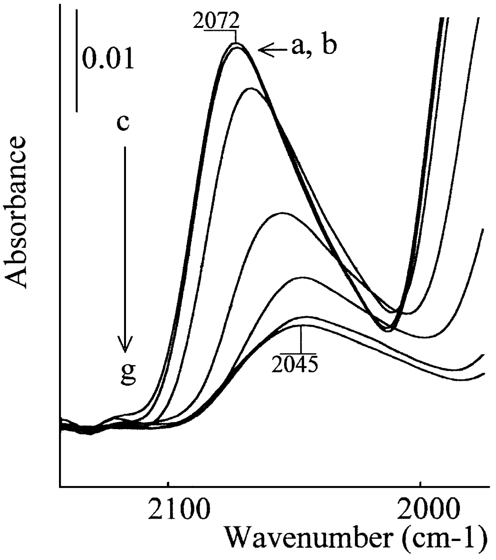

FIG. 2. Evolution of the IR band of the linearly adsorbed CO species with adsorption temperature: (a) 300 K, (b) 328 K, (c) 368 K, (d) 478 K, (e) 578 K, (f) 658 K, (g) 688 K.

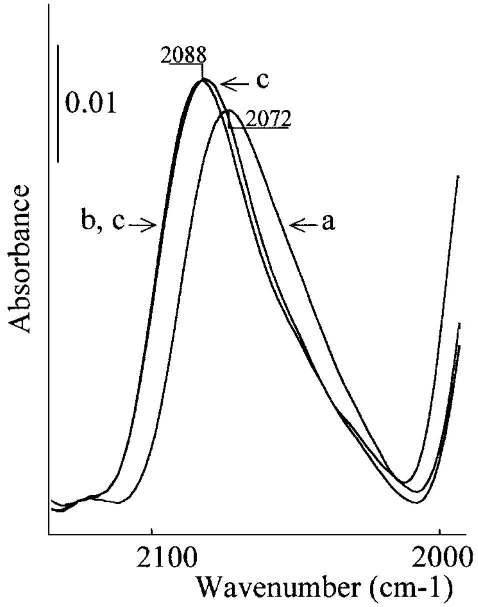

FIG. 3. Adsorption of CO (1% CO/He) at 300 K on 1.4% Pd/Al_2O_3: (a) reduced solid, (b) first adsorption of CO at 723 K followed by cool down to 300 K, (c) second adsorption of CO at 723 K followed by cool down to 300 K.

disproportionation reaction $2CO \rightarrow C + CO_2$ (29–31) does not change the number of palladium sites that adsorb the linear CO species. The disporportionation reaction is revealed, for temperatures higher than 523 K, by the appearance, in the recorded spectra, of three main IR bands at 1590, 1510, and 1390 cm^{-1} characteristic of carbonate species, adsorbed on the Al_2O_3 support. This reaction, however, creates some electronic changes (carbon deposition, low level of adsorbed oxygen, etc.) in the vicinity of the sites which leads to the observed shift in the IR band. Spectrum c in Fig. 3 is recorded after a second temperature increase up to 723 K (after spectrum b) followed by cooling down to room temperature. Spectra b and c show that there are no more changes in the Pd sites that adsorb the linear CO species, after the first treatment in CO/He.

As presented in a previous study (23) on Pt-containing solids, coverage of the sites by the linear CO species at a given temperature can be determined by assuming that the extinction coefficient of the IR band is constant with: (a) temperature; and (b) coverage, as studied by Rasband and Hecker (32) on Rh/SiO_2 catalysts. The ratio of the surface area of the IR band, at a given temperature, to the surface area of the IR band at 300 K provides the coverage of the sites at each temperature T, as shown in Fig. 4, curve a. Curve b in Fig. 4 was obtained after pretreatment of the solid following the experiments leading to curve a. Curves a and b confirm the stabilization of the catalyst and the reproducibility of the data. Note that the coverage is maintained at $\theta = 1$ over a short range of temperatures. To be sure that full coverage of the sites is really obtained with the 1% CO/He mixture, we ascertained at 300 K that the intensity of the IR band of the L species remains unchanged after the switch 1% CO/He → 5% CO/He. It must be noted that the accuracy of the surface area of the IR band for the L species is lower than in the preceding study on Pt/Al_2O_3 (23) ($\theta \pm 0.02$) due to the overlap of the IR bands of the linear and the bridged species. On Pt/Al_2O_3, the IR band of the linear CO species dominated the FTIR spectra.

c. Heat of Adsorption of Linear Species

Experimental curves a and b in Fig. 4 can be compared with the curve expected from Langmuir's model for adsorption without dissociation and given by

$$\theta = \lambda P/(1 + \lambda P). \qquad [1]$$

P is the pressure of adsorption and λ is the adsorption coefficient provided by statistical thermodynamics (23 and references therein) assuming the loss of three degrees of translation:

$$\lambda = \frac{h^3}{k * (2 * \pi * m * k)^{3/2}} * \frac{1}{T^{5/2}} * \exp\left(\frac{E_d - E_a}{R * T}\right), \qquad [2]$$

where h is Planck's constant, k is Bolztmann's constant, m is the weight of the molecule (28×10^{-3} kg/6.02×10^{23}), T is

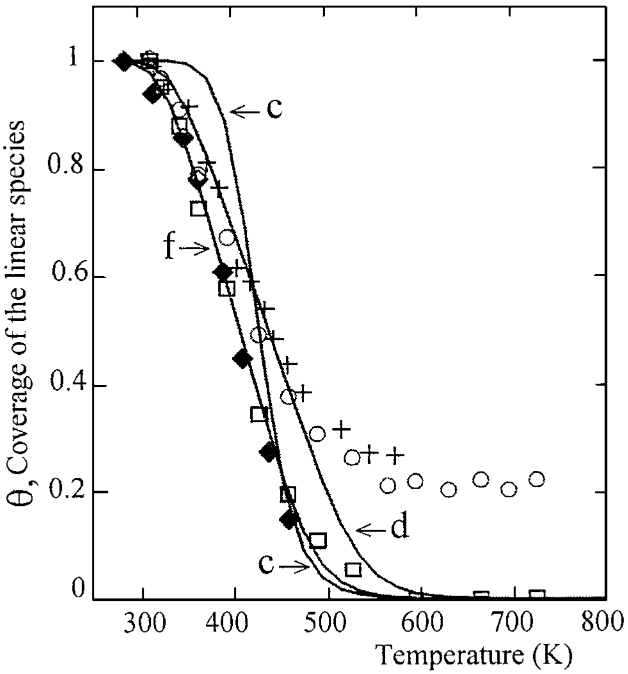

FIG. 4. Evolution in the coverage of the linearly adsorbed CO species: ○, (a) experimental data, first experiment; +, (b) experimental data, second experiment; (c) coverage according to Langmuir's model; (d) coverage according to expression [3] with $E_0 = 96$ kJ/mol and $E_1 = 58$ kJ/mol; □, (e) experimental data after correction (see text); (f) coverage according to expression [3] with $E_0 = 92$ kJ/mol and $E_1 = 54$ kJ/mol; ◆, (g) experimental data from Ref. (11).

adsorption temperature, E_d and E_a are the activation energies of desorption and adsorption, respectively, and $E_d - E_a$ is the heat of adsorption. Curve c in Fig. 4 provides the theoretical change in coverage according to expression [1] and assuming a heat of adsorption of 75 kJ/mol in expression [2]. The difference between the experimental data and the model is due to the fact that the heat of adsorption changes with the coverage of the surface as observed on various palladium-containing solids (6, 10, 11). Assuming a linear relationship between the heat of adsorption and the coverage of the sites θ is given by (23)

$$\theta = \frac{RT}{\Delta E} * \ln\left(\frac{1 + \lambda_0 * P}{1 + \lambda_1 * P}\right), \qquad [3]$$

where ΔE is the difference between the heats of adsorption at $\theta = 0$ (E_0) and $\theta = 1$ (E_1), and λ_0 and λ_1 are the adsorption coefficients at $\theta = 0$ and $\theta = 1$ according to expression [2]. Curve d in Fig. 4 provides the change in coverage according to expression [3] with the values $E_0 = 96$ K/mol and $E_1 = 58$ kJ/mol to fit the experimental curves. Note the agreement between the model and the experimental data over a large range of coverages ($\theta > 0.4$). A deviation, however, is observed for lower θ values. According to the above interpretation (the heat of adsorption increases with decrease in coverage) this deviation can be explained by considering that the heat of adsorption of the linear CO species ceases to follow a linear relationship with coverage at $\theta = 0.4$ and increases sharply. To explain that the coverage is almost constant above 573 K it must be assumed that the heat of adsorption is at least 165 kJ/mol. Another interpretation is that there are two linear CO species at the palladium surface with different heats of adsorption. The IR band of the first species, L_1, with a heat of adsorption <96 kJ/mol, dominates the FTIR spectra at low temperatures and overlaps the IR band of the second species, L_2, with a heat of adsorption higher than 165 kJ/mol. It is only when the coverage of L_1 species is very small (at high temperatures) that the IR band of the L_2 species dominates the FTIR spectra. As shown below, some data in the literature seem to support this interpretation.

Kuhn *et al.* (10) have used infrared reflection-absorption spectroscopy (IRAS) to study the adsorbed species on Pd(111) in the presence of CO pressure (10 Torr). The spectra are recorded as a function of decreasing temperature from 1000 K to temperatures lower than 300 K. At 1000 K only the bridged species is detected with an IR band at 1850 cm^{-1}. At around 720 K, a new IR band is detected at 2096 cm^{-1} attributed to a linear CO species. Its intensity increases to around 600 K and then remains almost constant until 300 K [for lower temperatures the evolution of the spectra is more complex; see Fig. 1 of Ref. (10)]. These observations indicate that: (a) a strongly adsorbed linear species is present on the surface (IR band observed at 700 K); and (b) the coverage of this species is almost constant in a large temperature range (600–300 K). This is in agreement with the characteristics of the supposed L_2 species on the present Pd/Al_2O_3 solid. In another study (11) the authors show the IRAS spectra of the adsorbed CO species on Pd/Ta(110). The palladium is deposited on Ta(110) by the evaporation of high-purity Pd wire. On these palladium sites and in the presence of gas-phase CO (range 10^{-9}–1 Torr) a single IR band (2053 cm^{-1} at 280 K and 10^{-6} Torr of CO) is observed and attributed to a linear CO species. The authors record the change in the intensity of this IR band as a function of the adsorption temperature at constant CO pressure. With the highest CO pressure (close to that used in the present study) the intensity decreases almost linearly in a large range of temperatures and the band disappears at around 480 K [see Fig. 3 of Ref. (11)]. This value is clearly lower than that found on Pd(111) (700 K) and indicates that the linear CO species detected on Pd(111) and Pd/Ta(110) have different heats of adsorption (even if the positions of their IR bands are similar). On Pd/Ta(110), the authors observe that the isosteric heat of adsorption of the L species, 92 kJ/mol at $\theta \approx 0$, decreases with increase in coverage according to a profile that is slightly different as compared with a straight line [see Fig. 6 of Ref. (11)]. The heat of adsorption at $\theta \approx 0$ is in good accord with the present results and finally Refs. (10, 11) lead to the conclusion that two linear CO species with different heats of adsorption may exist on the Pd particles. There are other data in the literature supporting the idea that two linear CO species are present on the Pd particles. It has been considered that on a 2% Pd/Al_2O_3 catalyst a single IR band for the linear CO species leads to two CO TPD peaks as measured with a mass spectrometer (28), indicating two adsorbed CO species of different activation energies of desorption. On a Pd/SiO_2 solid (15) the authors deconvolute an IR band located at 2090 cm^{-1} into two components. Some experimental data on the present solid also support the existence of two linearly adsorbed species. Figure 5 shows the FTIR spectra recorded during cool down in CO/He after the highest adsorption temperature (713 K). It can be observed that at 573 K a shoulder appears at 2075 cm^{-1} on the left side of the main IR band (2045 cm^{-1}) and its intensity increases with decrease in temperature. Finally, this IR band dominates the FTIR spectra (2088 cm^{-1} at 300 K, spectra c and d). The detection of the shoulder during cool down and not during heating can be ascribed to the surface change during the adsorption at high temperatures which leads later to the shift in the IR band of the L species to higher wavenumbers (as observed at 300 K in Fig. 3).

If we consider that two linear CO species, L_1 and L_2, are present on the Pd/Al_2O_3 solid, the evolution in the coverage of the first species L_1 with the lowest heat of adsorption can be obtained by subtracting the area of the IR band

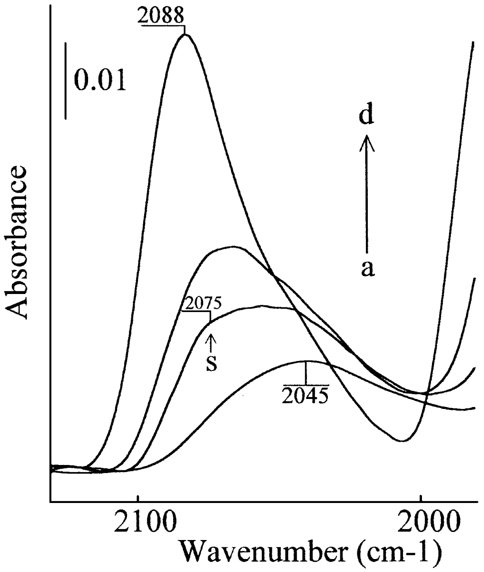

FIG. 5. Evolution of the IR band of the linearly adsorbed species in the course of the cooling in 1% CO/He: (a) 698 K, (b) 573 K, (c) 473 K, (d) 300 K.

recorded between 550 and 750 K from the total surface area of the IR band. This leads to curve e in Fig. 4. Assuming in Eq. [3] that $E_0 = 92$ kJ/mol and $E_1 = 54$ kJ/mol, then curve f is obtained in accord with the experimental data. Finally, curve g in Fig. 4 refers to the coverages obtained from the data of Kuhn *et al.* [Fig. 3 of Ref. (11)] on Pd/Ta(110) with a CO partial pressure of 130 Pa. Equation [3] fits curve g with $E_0 = 92$ kJ/mol. [value obtained in Ref. (11)] and $E_1 = 60$ kJ/mol. The good accord between the results of Kuhn *et al.* (11) and those of the present study confirms that the same adsorbed species are involved on Pd/Ta(110) as well as on the present Pd/Al_2O_3 solid. The interpretation of the evolution in the coverage for adsorption temperatures higher than 573 K (probably associated with a second linear CO species, L_2) requires more experimental data. It can, however, be noted that: (a) this section of the isobar of the L species corresponds to the decreasing section of the isobar of the bridged species as presented below (Fig. 12); and (b) according to the observations on Pd(111) (10), the L_2 species and the bridged CO species may be formed on the same plane.

Using ellipsometry spectroscopy Voogt *et al.* (24) studied the adsorbed species formed in the presence of gas-phase CO, in the temperature range 400–510 K, on Pd(111) and on Pt/SiO_2 solids [obtained by the evaporation of Pd on native SiO_2 layers formed on a commercial Si(100) wafer)]. Whatever the size of the Pd particles, they observed that the isosteric heat of adsorption decreases in a linear manner relative to the coverage from 148 kJ/mol at $\theta = 0.1$ to 90 kJ/mol at $\theta = 0.8$ (θ calculated using the ellipsometry signal). These values differ extensively from those used to fit the experimental data of Fig. 4 and also from those determined by Kuhn *et al.* (11). The results of (24), however, are in accord with those obtained for the bridged species (see below). This leads to the following remark: the highest CO pressure and the lowest temperature used by Voogt *et al.* are 1 Pa and 415 K, respectively. By inserting these values into expression [3] with the heats of adsorption used to fit the experimental data in Fig. 4, it is found that the highest coverage for the linear CO species in Ref. (24) is around $\theta = 0.01$. This indicates that there is not a significant presence of linear CO species on the surface under the experimental conditions of (24).

d. Change in Coverage of Bridged CO Species in Relation to Adsorption Temperature

Figure 6 shows the evolution of the IR bands of the bridged CO species alongside the adsorption temperature. At room temperature the IR band of the B_2 species (1942 cm^{-1}) dominates the FTIR spectrum. The increase in the adsorption temperature leads to a shift in the IR band of the B_1 species (i.e., 1980 cm^{-1} at 300 K and 1974 cm^{-1} at 368 K, spectra a and b, Fig. 6). This IR band overlaps with the one of the B_2 species at temperatures above 423 K. During this change, the total IR band surface area (both B_1 and B_2 species) is constant. This can be only interpreted as indicating that either the IR band of the B_1 species shifts with a constant intensity [this was previously observed on Pt-containing solids (23)] or that the sites adsorbing the B_1 species are converted into the sites adsorbing the B_2 species. However, this last interpretation seems improbable because after cooling down from 423 K to room temperature, in CO/He, the IR band of the B_1 species appears

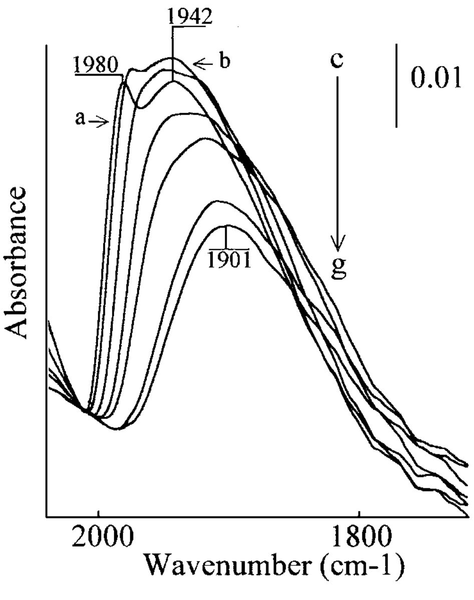

FIG. 6. Evolution of the IR band of the bridged CO species with adsorption temperature: (a) 300 K, (b) 368 K, (c) 443 K, (d) 518 K, (e) 568 K, (f) 658 K, (g) 688 K.

again as it does on the reduced solid. At temperatures higher than 443 K, the intensity of the remaining broad IR band decreases (Fig. 6, spectra d–g) whereas its position shifts to lower wavenumbers (i.e., 1942 cm^{-1} at 443 K, 1930 cm^{-1} at 518 K, 1917 cm^{-1} at 568 K, 1908 cm^{-1} at 658 K, and 1901 cm^{-1} at 688 K) according to a linear relationship with adsorption temperature. Figure 7 compares the spectrum recorded after CO adsorption at room temperature on the reduced solid (spectrum a) with the spectrum recorded after treatment in CO/He at 713 K followed by cool down to 300 K in CO/He (spectrum b). After adsorption of CO at high temperatures, a single IR band is observed at 1966 cm^{-1} (spectrum b) and its surface area is only slightly smaller than the surface area of the two IR bands of spectrum a. It appears that there is no significant modification of the number of sites that adsorb the bridged CO species (both B$_1$ and B$_2$) due to the disproportionation of CO at high temperatures. This reaction, however, leads to electronic site perturbations that eliminate the differentiation of B$_1$ and B$_2$ observed on the freshly reduced solid. Spectrum c in Fig. 7, recorded at room temperature after a second increase in CO/He at 700 K, shows that there is no further change in Pd sites. This means that if the disproportionation of CO continues during the second heating stage, the carbon deposition does not modify the adsorption sites. The site changes on the reduced solid are produced after 523 K because cooling down in CO/He from 523 K to room temperature leads to a spectrum similar to the initial spectrum (spectrum a, Fig. 7). Note that the disproportionation of CO is detected at this temperature as the appearance of the IR bands of the adsorbed carbonate species. The evolution, with adsorption temperature, of the coverage of sites adsorbing the bridged CO species (both B$_1$ and B$_2$ species) can be obtained using the ratio of the surface area of the IR band at temperature T and that at 373 K (full coverage). This leads to curve a in Fig. 8. Curve b corresponds to another experiment performed with a new catalyst pellet (after aging with CO/He treatment). Curves a and b in Fig. 8 prove the good reproducibility of the data.

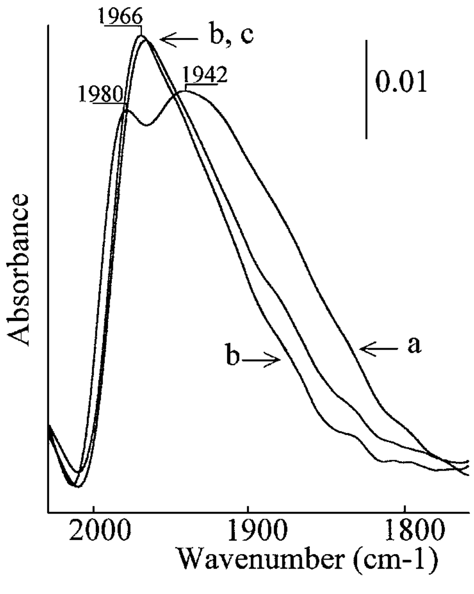

FIG. 7. Adsorption of CO (1% CO/He) at 300 K on 1.4% Pd/Al$_2$O$_3$: (a) reduced solid, (b) first adsorption of CO at 713 K followed by cool down to 300 K, (c) second adsorption of CO at 713 K followed by cool down to 300 K.

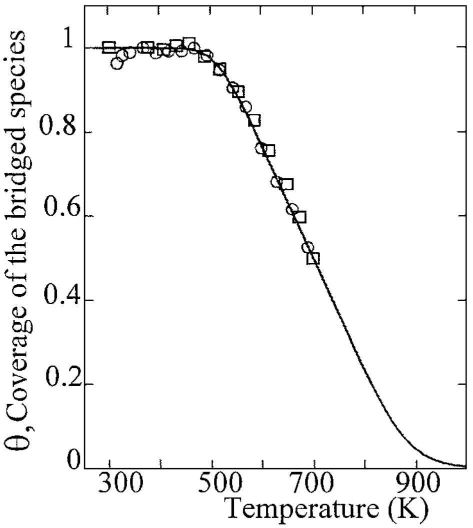

FIG. 8. Evolution in the coverage of the bridged CO species (both B$_1$ and B$_2$) on 1.4% Pd/Al$_2$O$_3$: □, (a) experimental data on the reduced solid; ○, (b) second set of experimental data with another catalyst pellet; —, (c) coverage according to Eq. [3] with $E_0 = 168$ kJ/mol and $E_1 = 92$ kJ/mol.

e. Heat of Adsorption of Bridged Species

As in the case for the linear CO species, expression [3] can be used to fit experimental curves a and b in Fig. 8. Curve c in Fig. 8 is obtained using $E_0 = 168$ kJ/mol and $E_1 = 92$ kJ/mol in expression [3]. Good agreement can be observed between the adsorption model and the experimental data.

The value $E_0 = 168$ kJ/mol can be compared with the data on monocrystals, in the literature, which form mainly bridged CO species (3–5). As indicated in the Introduction, the heats of adsorption of CO are not markedly dependent on the oriented planes [range: ≈140 to ≈170 kJ/mol (6–9, 27)]. The B$_1$ and B$_2$ species are considered to be situated on Pd(100) and Pd(111), respectively (15–17, 19). On monocrystals the initial heats of adsorption on these oriented faces are very close. On Pd(111) and Pd(100) Bradshaw and Hoffmann (27) report 140 and 150 kJ/mol, respectively, in accord with the values of Conrad *et al.* (6) and Doyen and Ertl (33). These values are in accord with $E_0 = 168$ kJ/mol as found above. Szanyi and Goodman (34) have used the IRAS method to study CO chemisorption on Pd(100). They record the evolution of coverage of the adsorbed species with adsorption temperature over several isobars (range: 10^{-7}–10^{-4} Torr) and determine the isosteric heats of adsorption at various coverages. They observe (34) a linear decrease in the heats of adsorption with coverage from 161 kJ/mol at $\theta = 0.05$ to ≈130 kJ/mol at $\theta = 0.4$. The relationship observed between the heats of adsorption and the coverage as well as the values determined are in good accord with those of the present study (164 kJ/mol at $\theta = 0.05$ and 138 kJ/mol at $\theta = 0.4$). It is to be noted that, in our case, the heat of adsorption corresponds to an average of those of two species, B_1 and B_2 (with a higher contribution of the B_2 species which dominates the FTIR spectra), whereas on the oriented planes a single species is involved. The fact that an adsorption model assuming a single adsorbed species (expression [3]) fits the experimental curves involving two adsorbed species indicates that the heats of adsorption of the two species are very close and this is in agreement with the data on oriented planes (6, 27, 33). Moreover, it is demonstrated below that modification of the ratio between the B_1 and B_2 species has no influence on the heats of adsorption. In another study (35) the authors apply the same experimental procedure to study the heat of adsorption of CO on Pd(111). A linear decrease in the heats of adsorption with an increase in coverage is also observed from 146 kJ/mol at $\theta = 0.005$ to 103 kJ/mol at $\theta = 0.3$. The relationship observed as well as the values at low coverages (35) is in accord with the results of the present study.

The heat of adsorption $E_0 = 168$ kJ/mol can be compared with the results on Pd-supported solids, in particular those obtained under experimental conditions similar to those of the present study (during adsorption) but using ellipsometry spectroscopy as the analytical method (24). The authors determine the isosteric heats of adsorption of CO on Pd(111) and on Pd/SiO_2 solids with different particle sizes (24). We showed above that under the experimental conditions of (24), linear adsorbed species can be present on the Pd surface but at a very low coverage. For Pd(111) the authors observe that the isosteric heats of adsorption decrease with coverage according to a linear relationship from 145 kJ/mol at $\theta = 0.15$ to 95 kJ/mol at $\theta = 0.7$ (coverage determined with ellipsometry signal). Assuming the same relationship in the range 0–0.15, the heat of adsorption at $\theta = 0$ is around 160 kJ/mol. The same data are observed for Pd/SiO_2 solids with particle size in the range 9.5–1.5 nm. It must be noted that the authors (24) found that the decrease in heat of adsorption with increase in coverage is affected by particle size, but they believe that this is probably due to the presence of small undetectable amounts of contamination of the surface of the palladium particles. It appears that the E_0 value in the present study for the bridged species and that found in Ref. (24) are in very good accord, even if the Pd-containing solids have different compositions and structures. Another comparison involving Pd-supported catalysts can be made with studies using microcalorimetric measurements. It must be taken into account that under these experimental conditions both linear and bridged CO species can be present on the surface. On a 2.2% Pd/SiO_2 solid (22), the heat of adsorption at $\theta \approx 0.1$ is 135 kJ/mol. This value is smaller than the value found in the present study for bridged species (160 kJ/mol at $\theta \approx 0.1$). The difference can be explained by the contribution of the L_1 species to the heat of adsorption. This species can be present at a low coverage (see below) with a heat of adsorption of 92 kJ/mol. Chou and Vannice apply a microcalorimetric method to measure, at room temperature, the heats of adsorption of CO at high coverages, on various Pd-containing solids (9). The authors use 75 Torr of CO in an inert gas and they consider that the reversible fraction of the adsorbed CO is not taken into account. Only the heat of adsorption of the irreversible adsorbed CO species is determined. This irreversible fraction is probably composed of bridged CO species (B_1 and B_2) and a fraction of the linear CO species. In a large range of particle sizes and on several Pd-supported solids, the heat of adsorption at high coverage is 96 kJ/mol. This value is in good accord with $E_1 = 92$ kJ/mol used to obtained curve c in Fig. 8. Note that the value of Chou and Vannice probably corresponds to the sum of the heats of adsorption (a) of the bridged CO species at high coverages and (b) of the irreversible fraction of the L species at room temperature, i.e., at low coverages (see below) when the value is around 92 kJ/mol.

It appears that the experimental procedure described in the present study, associated with an adsorption model assuming a linear decrease in the heats of adsorption with increase in coverage, leads to determination of the heats of adsorption of each adsorbed species (linear and bridged) at various coverages. It is shown below that modification of the B_1/B_2 ratio has no effect on the heat of adsorption. This means that the B_1 and B_2 species have comparable heats of adsorption (in accord with the data on oriented planes) which cannot be differentiated under the present experimental conditions. The results presented above agree with the data on oriented planes as well as on model particles. Taking into account the diversity of the palladium-containing solids involved in the comparison, it seems difficult to consider that the heats of adsorption are strongly modified by certain parameters such as the support of the catalyst and the metal dispersion.

In the following section some experimental data are presented in relation to the heats of adsorption of the adsorbed species: (a) various pretreatments of the solid; (b) desorption of the adsorbed species at room temperature; and (c) sintering of the Pd particles.

f. Thermal Treatment in He after Reduction

In the above results, the catalyst is cooled down to room temperature in hydrogen after its reduction and helium is then introduced for 10 min before CO chemisorption. In the literature, the Pd-supported catalysts are often

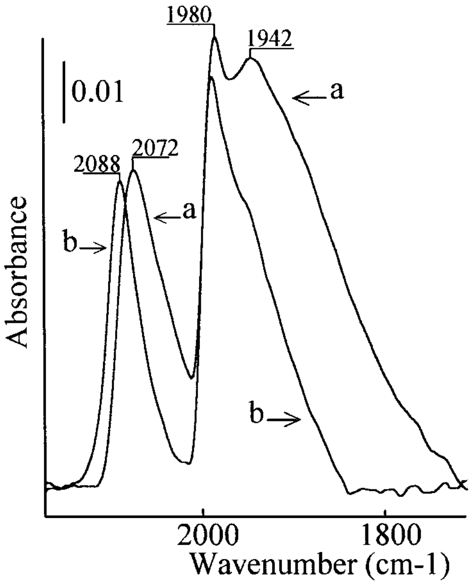

FIG. 9. FTIR spectra at 300 K of the adsorbed CO species (1% CO/He) after different pretreatments of the Pd/Al$_2$O$_3$ solid: (a) reduction at 713 K and cool down in hydrogen, (b) reduction at 713 K followed by 30 min in helium and cool down in helium.

treated in an inert atmosphere (vacuum or inert gas) at the reduction temperature before CO chemisorption at room temperature (12, 14–16). After this treatment, the IR band of the linear CO species is detected at around 2085 cm^{-1} while the IR band of the B$_2$ species is detected in the form of a shoulder of the IR band of the B$_1$ species and not as the main IR band (as in Fig. 1). Figure 9 compares the FTIR spectra after adsorption of CO at room temperature on a solid pretreated according to two procedures: spectrum a is recorded on the solid reduced at 713 K and cooled down in hydrogen, and spectrum b is recorded on the solid reduced and then treated for 30 min in helium at 713 K and cooled down to 300 K in He. Spectrum b is very similar to those found in the literature for the same pretreatment of the solid. It can be observed that: (a) the IR band of the L species shifts to higher wavenumbers (2088 cm^{-1}) after the helium treatment but without any change in its intensity; (b) the IR band of the B$_2$ species is strongly decreased (recorded in the form of a shoulder of the IR band of the B$_1$ species); and (c) the intensity and the position of the IR band for the B$_1$ species are only slightly affected by helium treatment. Note that the position of the IR band of the L species after helium treatment is similar to that observed in Fig. 3 (solid cooled in CO/He after adsorption at high temperature). It is not within the scope of the present paper to discuss an accurate explanation of the observed differences between spectra a and b in Fig. 9. However, before presentation of the heats of adsorption of the linear and bridged species detected in spectrum b in Fig. 9, different experiments are described to provide a possible explanation.

The helium treatment at high temperatures after the reduction step is performed with the objective of removing the adsorbed hydrogen. However, if hydrogen is present on the surface at room temperature, it is known that CO chemisorption leads to displacement of the chemisorbed hydrogen (13 and references therein). Moreover, it has been observed (13) that adsorbing CO with either a CO/He or a CO/H$_2$ mixture does not modify the intensities of the IR bands of the CO species adsorbed on various Pd-supported solids. In the presence of hydrogen a downshift of the IR bands is, however, sometimes observed (13). Taking into account the experimental procedure followed in the present study (cool down in hydrogen), it can be considered that: (a) CO displaces a fraction of the chemisorbed hydrogen (the intensities of the IR band of the L species are comparable in spectra a and b in Fig. 9; and (b) the remaining adsorbed hydrogen leads to the downshift of the IR band of the L species (2072 cm^{-1} in spectrum a compared with 2088 cm^{-1} in spectrum b, Fig. 9). It is, however, difficult to explain how the remaining hydrogen increases the quantity of the B$_2$ species (compare spectra a and b in Fig. 9). We have thus considered that helium treatment at high temperatures may lead to contamination of the surface with small traces of O$_2$ and some experiments have been performed to support this idea and to study the effects on the observed spectra of the presence of few parts per million of O$_2$ in the helium flow. Spectrum a in Fig. 10 was obtained after adsorption of 1% CO/He at room temperature on the solid cooled down in H$_2$. Spectrum b is recorded after the following steps: spectrum a → 100 ppm O$_2$/He (1 min) → 1% CO/He. It can be observed that after O$_2$ treatment: (a) the IR band of the L species shifts to higher wavenumbers (2072 cm^{-1} → 2083 cm^{-1}) without any decrease in its intensity; and (b) the IR bands of the bridged species are not modified. The observed displacement can be interpreted either as the adsorption of O$_2$ on the surface or/and as the removal by O$_2$ of the remaining adsorbed hydrogen. Spectrum c in Fig. 10 was recorded according to the following procedure: H$_2$ (713 K) → H$_2$ (300 K) → He (300 K, 10 min) → 100 ppm O$_2$/He (300 K, 5 min) → He (10 min) → 1% CO/He. It can be observed that: (a) the IR band of the L species shifts to higher wavenumbers (2072 cm^{-1} → 2090 cm^{-1}) but its intensity is only slightly reduced; (b) the intensity of the IR band of the B$_2$ species (1942 cm^{-1}) is strongly reduced (it is detected as a shoulder of the IR band of the B$_1$ species); and (c) the IR band of the B$_1$ species is not modified by O$_2$ treatment. Note that after oxygen treatment at room temperature, the spectrum (Fig. 10c) is similar to that observed after treatment in helium at high temperatures (Fig. 9b). This shows that it cannot be ruled out that the Pd surface can be contaminated with small amounts of oxygen present in the helium gas. Taking into account the time needed to cool down the solid in helium from 713 K to room temperature (≈2 h) and

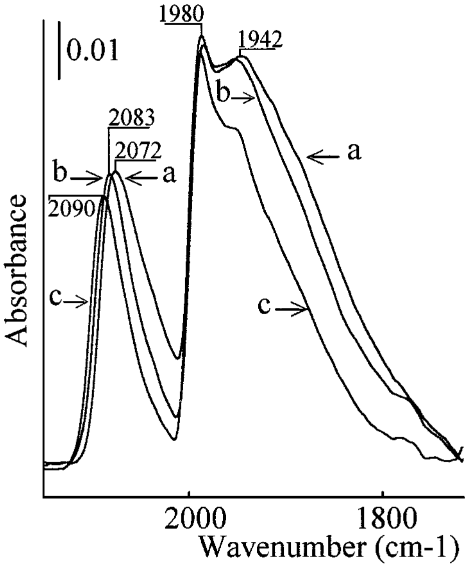

FIG. 10. Change in the FTIR spectra of the adsorbed CO species at 300 K through the presence of low levels of oxygen: (a) solid pretreated and cooled down in hydrogen to room temperature; (b) spectrum (a) → 100 ppm O_2/He (1 min) → 1% CO/He; (c) solid pretreated → H_2 (300 K) → He (10 min) → 100 ppm O_2/He (5 min) → He (10 min) → 1% CO/He.

assuming that the reduced Pd surface adsorbs all the O_2 traces, the contamination created with the 100 ppm O_2/He mixture can be observed through the presence of less than 1 ppm of O_2 in the helium gas. This contamination can be produced by the effusion of O_2 through very small leaks at the swagelok unions between the purification traps (O_2, H_2O) and the IR cell. We have not tried to solve this possible contamination because, as shown below, helium treatment at high temperatures in the end does not affect the heats of adsorption of the adsorbed species. Note that it will be shown in a coming study that the ratio of the B_1 and the B_2 species can be modified by the preparation of various Pd-containing solids leading to spectra similar to spectrum b in Fig. 9 but recorded after cool down in hydrogen after the reduction.

Figure 11 shows the evolution of the FTIR spectra with the increase in adsorption temperature on a reduced solid that is then treated in helium at 713 K. The intensity of the IR band of the L species decreases progressively after 330 K and its position shifts to lower wavenumbers (2090 cm^{-1} at 300 K, 2082 cm^{-1} at 363 K, 2063 cm^{-1} at 458 K, 2046 cm^{-1} at 585 K, and 2044 cm^{-1} at 703 K) according to a linear relationship in the temperature range 340–585 K. The evolution of the IR band of the bridged species is more complex. At room temperature (spectrum a) the IR band of the B_1 species (1985 cm^{-1}) dominates the FTIR spectrum. The increase in temperature leads: (a) to an increase in the shoulder due to the B_2 species until 473 K; and (b) to the shift in the IR band of the B_1 species (1985 cm^{-1} at 300 K, 1981 cm^{-1} at 363 K, 1963 cm^{-1} at 458 K) but without a significant decrease in its intensity. At temperatures higher than 458 K, the intensity of the broad IR band (Fig. 11, spectrum d) decreases progressively with the increase in adsorption temperature (1917 cm^{-1} at 585 K and 1903 cm^{-1} at 703 K). Note that the results in Fig. 11 are very similar to those in Figs. 2 and 6. The main difference is the increase in the IR band of the B_2 species between 300 and 458 K. In another experiment, after the solid is heated in 1% CO/He from room temperature to 470 K, it is cooled down to 373 K in CO/He. It is observed that the surface area of the IR band of the bridged species remains constant during the cooling. This means that the modifications of the palladium surface revealed by the increase in the B_2 species IR band are irreversible.

The evolution in coverage of the adsorbed species (L and both B_1 and B_2) with adsorption temperature can be obtained using the procedure described above. For the bridged species, the surface area of the IR band at 473 K is used to determine full coverage. Curves a and b in Fig. 12 respectively provide the evolution in the coverages of the linear and bridged CO species during the heating from 300 to 500 K. For linear CO species, the curve is similar to that determined on a solid cooled down in hydrogen (curve e in Fig. 12). This means that the heat of adsorption of the L_1 species is not affected by cooling down either in hydrogen or in helium. The differences in Pd sites created by the two treatments (presence of chemisorbed hydrogen, contamination of the surface with tiny O_2 traces) have no effect on the heat of adsorption of the L_1 species. For the bridged CO species, curve b corresponds to the increase in the number of sites adsorbing the B_2 species, as described in Fig. 11. After the experiments leading to curves a and b, the solid is cooled down to 390 K in CO/He and then the

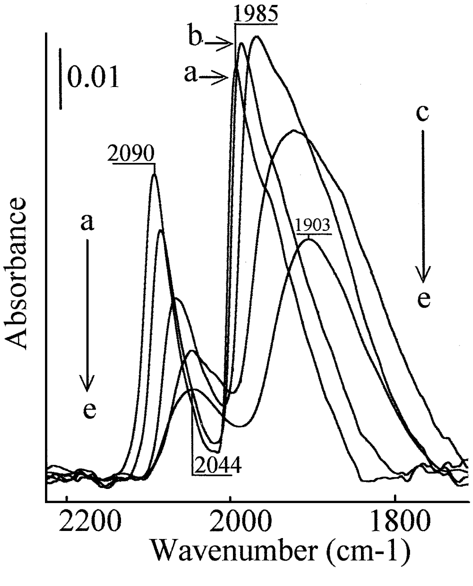

FIG. 11. FTIR spectra of the adsorbed CO species as a function of adsorption temperature on a helium-treated solid: (a) 300 K; (b) 363 K; (c) 458 K; (d) 585 K; (d) 703 K.

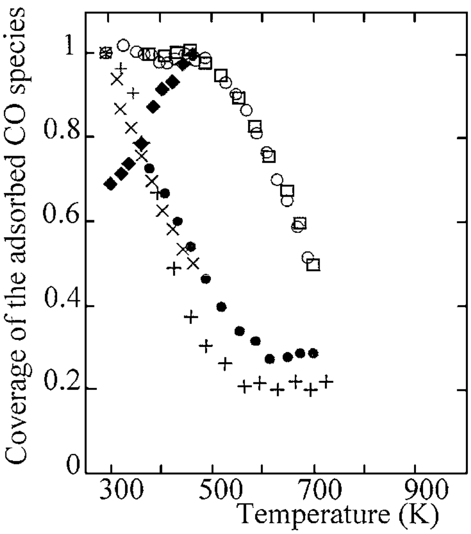

FIG. 12. Evolution in the coverages of the linear and bridged CO species with adsorption temperature: ×, (a) and ◆, (b) coverages of the linear and bridged CO species, respectively, after cool down of the Pd/Al_2O_3 solid in helium (highest adsorption temperature 475 K); ●, (c) and □, (d) coverage of the linear and bridged CO species, respectively, after the experiment with curves a and b (see text for more details); +, (e) and ○, (f) coverage of the linear and bridged CO species, respectively, after cool down of the solid in hydrogen.

temperature is increased again to 713 K. Curves c and d in Fig. 12 provide the evolution in the coverages of the linear and bridged CO species, respectively, during this experiment. For the L_1 species there is no difference with curves a and e. For the bridged species, curve d is similar to that (curve f, Fig. 12) obtained after cool down in H_2 (same as curve a in Fig. 8). This indicates that the heats of adsorption of the bridged CO species are also independent with respect to the pretreatment of the solid (cool down either in hydrogen or in helium). The above experiments lead to the following comments: (a) the heat of adsorption of the linear CO species is independent of the position of its IR band at 300 K (2090 or 2072 cm^{-1}); and (b) the heat of adsorption of the bridged species (both B_1 and B_2) is independent of the proportion of the two bridged species (see Fig. 9). The latter comment confirms that the heats of adsorption of the B_1 and B_2 species are very close. Note that it is mainly because the surface area of the IR band of the B_2 species was constant during the increase in adsorption temperature from 300 to ≈500 K (Fig. 8) after cool down in hydrogen (see Fig. 8) that we have proceeded with this experimental procedure. In relation to possible contamination of the Pd surface, hydrogen can be considered to protect the surface from O_2 contamination.

g. Aging of Solid with CO/He Treatment at High Temperatures

Spectrum a in Fig. 13 was recorded at room temperature in 1% CO/He after pretreatment of the solid followed by cool down in H_2. Note that IR bands were detected at 2080, 1985, and 1932 cm^{-1} for L_1, B_1, and B_2 species, respectively. Spectrum b was recorded after heating in CO/He at 713 K followed by cool down in CO/He (IR bands at 2085, 1973, and 1947 cm^{-1}). Spectrum c was recorded after the second reduction of the solid at 713 K after spectrum b (IR band at 2072, 1980, and 1942 cm^{-1}). Spectrum c is similar to that in Fig. 2 after two adsorption/pretreatment cycles. Comparison of spectra a and c in Fig. 13 shows that qualitatively the species formed after adsorption of CO are identical on the fresh solid and aged solid but the intensities of the IR bands are higher on the fresh solid. The irreversible surface modifications are due to the initial treatment in CO/He at high temperatures (spectrum b) (the intensities of the IR bands of the L species are comparable in spectra b and c in Fig. 13). Note that the intensity of the IR band of the B_1 species is almost not affected by aging while the intensities of the IR bands of the B_2 species and the linear CO species decrease. Spectrum c is not strongly modified by two successive adsorption/pretreatment cycles. Aging of the catalyst is, however, clearly observed by comparing the spectrum recorded after one cycle (spectrum c in Fig. 13) with that recorded after several cycles (≈20, spectrum d in Fig. 13). The intensities of the IR bands of the L and B_2 species are more strongly affected than the intensity of the IR band of the B_1 species. After 20 cycles, the surface area of the IR band of the L species decreases by 45% and the area of the bridged species (both B_1 and B_2) by 25% compared with the second cycle (spectrum c). It seems that there is a correlation between the L and B_2 species which decrease similarly with aging of the solid. For the linear CO species we have studied the change in its coverage on a fresh catalyst

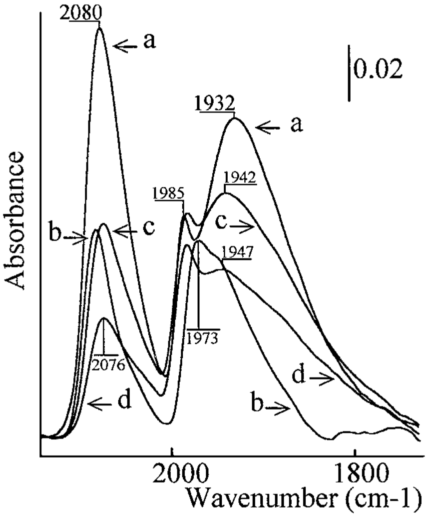

FIG. 13. Adsorption of CO at 300 K on various pretreated solids: (a) freshly reduced solid (first treatment); (b) cooled down to room temperature after adsorption at 713 K; (c) second reduction of the catalyst; (d) reduced solid after 20 adsorption/pretreatment cycles.

during an increase in temperature to 473 K. This adsorption temperature limits the modifications of the palladium surface observed after cool down to 300 K in CO/He. We have observed the same linear decreasing profile $\theta = f(T)$ as observed on the aged solid. This indicates that there is no change in the heats of adsorption of the L_1 species with aging of the catalyst. Moreover, the heats of adsorption on L and B species are not modified after ≈20 cycles of adsorption/pretreatment, even if the linear/bridged species ratio is modified. Assuming that aging of the catalyst is due to sintering of Pd particles, it appears that the increase in particle size does not modify the heats of adsorption of L and B species. The main difference observed between the curves giving $\theta = f(T)$ with aging of the solid is the increase in the coverage limit of the linear species (L_2 species) from 0.2 to 0.34 after ≈20 cycles. This indicates modification of the L_1/L_2 species ratio.

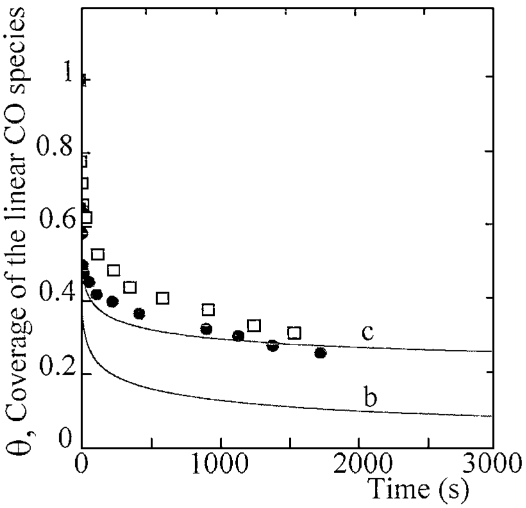

FIG. 14. Evolution in the coverage of the linear CO species during desorption in helium at 300 K: □, (a) experimental data, flow rate of helium (200 cm^3/min); (b) curve using expression [4] with $E_1 = 58$ kJ/mol and $E_0 = 96$ kJ/mol; (c) assuming the presence of the second L_2 species; ●, (d) experimental data, flow rate (2000 cm^3/min).

h. *Isothermal Desorption of Adsorbed Species at Room Temperature*

Many studies (12, 14–16) note that the intensity of the linear CO species adsorbed on palladium atoms decreases at room temperature in the course of an inert treatment (vacuum or inert gas), while bridged species are not affected [or slightly decreased (14)]. The fraction of adsorbed CO species removed from the surface is called reversible, or weakly adsorbed. In particular, Sheu *et al.* (14) underline the necessity of desorbing at least 50 min in argon after CO chemisorption on reduced Pd/SiO_2 solids, to obtain a significant relationship between the ratio of intensity of the IR band of the B species/intensity of the IR band of the L species and dispersion of the palladium particles. These results can be explained more quantitatively taking into account the heats of adsorption determined above for L and B species.

We have studied the change in IR bands according to the following experiment (performed on a solid treated in helium at 713 K after H_2 reduction under experimental conditions similar to those in the literature): after CO chemisorption at 300 K, a switch is made to a helium flow (200 cm^3/min). The IR spectra (not shown) recorded during the desorption in helium indicate that the intensity of the bridged CO species IR band (spectrum a, Fig. 11) is not significantly modified while the IR band of the L species decreases and shifts to lower wavenumbers (from 2090 cm^{-1} at $t = 0$ to 2074 cm^{-1} after 25 min of desorption). Figure 14, curve a, indicates the evolution in coverage of the L species with time on stream in helium. This experimental curve can be compared with that obtained from the following desorption model. Taking into account that the adsorption of CO is not activated, it can be considered that the activation energy of desorption varies with coverage by the same relationship as the heat of adsorption. Assuming first order for desorption of the L species, the evolution in coverage θ with time of desorption t is given by

$$\frac{-d\theta}{dt} = \frac{kT}{h} * \exp\left(-\frac{E_{\mathrm{d}}(\theta)}{RT}\right) * \theta, \qquad [4]$$

with E_{d} varying according to a linear relationship from 54 kJ/mol at $\theta = 1$ to 92 kJ/mol at $\theta = 0$. Figure 14 (curve b) provides the evolution in coverage using expression [4]. There is qualitative accord with the experimental data but the coverage obtained after 25 min on stream is lower on curve b than on curve a. An improved correlation is obtained considering the following remark. To interpret the evolution in coverage of the L species at $T_{\mathrm{a}} > 563$ K (Fig. 4), we have considered that there is probably a second L_2 species with a heat of adsorption higher than 165 kJ/mol. Figures 4 and 12 show that this species leads to a coverage limit in the range 0.2–0.3 according to the aging of the solid. Curve b can be modified considering that: (a) this second species is present at 300 K; and (b) it does not desorb during the experiment concerning curve a. Curve c, obtained assuming that the L_2 species contributes to the coverage for 0.23, leads to better accord with curve a. It can, however, be observed that the experimental curve a is higher than curve c, particularly at the beginning of the desorption ($t < 400$ s). We believed that this difference is produced by the readsorption of CO due to residual CO pressures in the IR cell and, in a second experiment, we increased the helium flow rate from 200 to 2000 cm^3/min (curve d, Fig. 14). Curve d is now close to theoretical curve c. This shows the difficulty in determining, on metal-supported catalysts, the energetic factors linked to chemisorption through a procedure involving a desorption step. Various phenomena, in particular readsorption and mass transfer (20, 21), may influence the results. Note that: (a) expression [4] can almost fit curve a assuming an activation energy of desorption of 75 kJ/mol at $\theta = 1$; and (b) the results of Fig. 14 show that the relationship between the heats of adsorption and the coverage determined under adsorption equilibrium conditions at high temperatures provides a good representation of a desorption process at room temperature.

The above results allow us to quantify the problem of the desorbing fraction of the linear CO species at 300 K. The main conclusion is that reversible and irreversible L species are adsorbed on the same sites. It is only the relationship between the activation energy of desorption (or the heat of adsorption) and coverage that determines their respective fractions after a given time of desorption. The results in Fig. 14 underscore the remarks of Sheu *et al.* (14) on the desorption procedure. It can be understood that to establish a valid correlation between the ratio intensity of the IR band of the B species/intensity of the IR band of the L species and the dispersion of Pd particles, it is necessary to desorb for a long enough time to obtain almost constant coverage of the linear species (more that 30 min); otherwise the coverage could be different from one experiment to another. As this coverage is a function of the relationship between the activation energy of desorption and coverage, it must be assumed that the heat of adsorption is not modified by particle size and this seems verified by (9, 36) and by the present results (see below). Note that expression [4] shows that an increase of 10 kJ/mol in activation energy at low coverages increases significantly the final coverage from 0.3 to 0.45 after 30 min of desorption. Another experimental procedure [with the objective of Ref. (14)] is to remain at adsorption equilibrium, at the full coverage of the linear and bridged CO species.

The heats of adsorption of the bridged CO species determined above (168 kJ/mol at $\theta = 0$ and 92 kJ/mol at $\theta = 1$) introduced into expression [4] indicate that the theoretical coverage after 30 min of desorption is $\theta = 0.92$. This value is in accord with the different observations in the literature on the strong stability of bridged species in inert atmosphere, at room temperature, and with the results of the present study.

i. Heats of Adsorption of CO on Palladium-Supported Solids and Particle Sizes

After the first reduction of the 1.4% Pd/Al_2O_3 catalyst the amount of chemisorbed CO at room temperature is 32 μmol CO/g of catalyst, which leads to a dispersion of 24% assuming $CO/Pd_s = 1$ as considered by Rieck and Bell (29) and Chou and Vannice (9). This dispersion is similar to those found in the literature on Pd/Al_2O_3 catalysts (for similar metal loading and reduction temperature). For instance, in (9) for a reduction temperature of 673 K the dispersions are 27 and 30% on 1.8 and 2.3% Pd/Al_2O_3 catalysts, respectively, leading to a particle size of around 3 nm, and in (2) for the same reduction temperature the dispersion is 27% on 1.9% Pd/Al_2O_3, leading to a particle size of 4 nm. We have shown that the increase in the number of adsorption/pretreatment cycles leads to a decrease in the intensities of the IR bands of the L and B species (Fig. 13). This has been ascribed to the sintering of Pd particles and we have shown that this aging has no influence on the heats of adsorption of the different adsorbed CO species. The fact that the heats of adsorption are not influenced by the increase in particle size is in agreement with the results of Chou and Vannice (9) using microcalorimetric measurements. They observed on several Pd-supported catalysts that the heat of adsorption of CO at high coverages is almost constant with palladium particle size for values higher than 3 nm and increases sharply for lower values. These results have been confirmed by Henry *et al.* (36) using another experimental procedure on Pd/MgO model catalysts. Voogt *et al.* (24) conclude that there is no particle size effect in the range 1.5–9.5 nm on Pd/SiO_2 model catalysts. The same conclusion was made in an early study on $Pd/\alpha\text{-}Al_2O_3$ model catalysts (37) for particle sizes in the range 1.5–8 nm. In the two studies (24, 37) the results concern adsorbed species with the highest heats of adsorption (B species). The present results confirm the above conclusions and in addition they show that this is true for the heats of adsorption of L_1 (see below) and B species. Note that Ladas *et al.* (37) concludes to the remarkable structure insensitivity of CO chemisorption (bridged species) on Pd because the heat of adsorption of this species was not strongly dependent on the exposed planes.

Another conclusion of Chou and Vannice (9) and Henry *et al.* (36) related to the effects of particle size on heat of adsorption (at high coverages) is the strong increase in this parameter for particles smaller than 3 nm. Assuming that the decrease in particle size increases the number of low-coordinated palladium atoms (adsorbing linearly CO), and taking into account the heats of adsorption found for L_1 species (varying from 92 kJ/mol at $\theta = 0$ to 54 kJ/mol at $\theta = 1$) and bridged CO species (varying from 168 kJ/mol at $\theta = 0$ to 92 kJ/mol at $\theta = 1$), it seems at first sight difficult to interpret the increase in the heats of adsorption for particle sizes smaller than 3 nm. It can be considered, as did Voogt *et al.* (24), that the observations in (9, 36) are related either to some surface contamination with tiny traces of impurities or to a support effect. However, we showed above (Fig. 10) that contamination with O_2 can lead to some modifications in the FTIR spectra but does not influence the heats of adsorption of linear and bridged CO species. In agreement with the above comment, some studies (38, 39) on Pd/Al_2O_3 model catalysts (Al_2O_3 crystals) indicate that the ratio of the surface areas of two TPD peaks noted α_1 and α_2 at low and high temperature, respectively, increases with the decrease in particle size [lowest value 2.5 nm in (38)]. The TPD peaks are ascribed to a linear CO species [α_1, activation energy of desorption: 93.4 kJ/mol with $\nu = 10^{13}\ s^{-1}$ (38)] and to bridged CO species [α_2, activation energy of desorption: 135 kJ/mol at $\theta = 0.02$, with $\nu = 10^{13}\ s^{-1}$ (38)]. For a particle size of 27 nm, the α_1 peak is very weak (38) and the TPD spectra are similar to those observed on Pd(111). However, the correlation between the present results and the conclusions of Refs. (9, 36) can be obtained considering the second linear CO species L_2 detected at high temperatures (Figs. 4 and 12). We have shown that its heat of adsorption must be higher than 165 kJ/mol to explain its presence during the adsorption at 713 K. Using the same experimental procedure, we determined (23) on platinum-supported solids that the heat of adsorption of a linear CO species is ≈ 200 kJ/mol at low coverages. This value is sufficient to explain the observed increase in the heats of adsorption in Refs. (9, 36). It must be assumed that either the L_1/L_2 ratio or the B/L_2 ratio decreases for particles sizes smaller than 3 nm. Note that under the present experimental conditions it was not possible to determine exactly the heat of adsorption of this L_2 species at various coverages. Moreover, the supposed increase in the amount of L_2 species with the increase in dispersion seems to be in accord with the results of Zilm *et al.* (40). Using NMR spectroscopy, they observe that the mobility of the CO species on 56% dispersed Pd particles (mainly linear CO species) is greatly reduced in comparison to that on catalysts with 16–19% dispersions.

The discrepancy between the studies (either decrease or increase in the heat of adsorption of CO for particle sizes smaller than 2–3 nm) seems to be linked to the location of Pd sites that adsorb the L_1 and L_2 species. We have mentioned that the heats of adsorption of the L_1 species provides a curve $E = f(\theta)$ in accord with the values of Kuhn *et al.* (11) on Pd/Ta(110) obtained using IRAS analysis [see also Ref. (19) of (11) on Pd/W(110)]. Kuhn *et al.* underscore the fact that the preference for linear bonding sites on Pd/Ta(110) (compared with oriented planes which form mainly bridged CO species) is an effect induced by the interactions between the metal adlayer and the substrate. Sellidj and Koel (41) have studied in detail this interaction on Pd/Ta(110) with various Pd loadings. They determined the changes in the desorption activation energies (TPD) and HREELS spectra of adsorbed CO species as a function of the coverage θ_{Pd} of the palladium layer. On Pd annealed layers, they showed (41) that for $\theta_{\mathrm{Pd}} \leq 1$ [pseudomorphic and fcc(111) monolayers] only a linear CO species is formed whatever the coverage of CO (energy loss at 2090 cm^{-1}), with a desorption activation energy of 64 kJ/mol ($\nu \approx 5 \times 10^{13}\ s^{-1}$) at $\theta \approx 0$. The authors believe that the fcc(111) structure is reconstructed to pseudomorphic structure on exposure to CO. For $\theta_{\mathrm{Pd}} = 3$, after annealing at 550 K (Pd clusters formed on top of the Pd monolayer) only the bridged CO species (energy loss at 1950 cm^{-1}) is observed at low exposures while linear CO as well as bridged CO species are detected at high exposures. This study (41) clearly indicates that a linear CO species with a low heat of adsorption is preferentially formed on a Pd monolayer while a bridged CO species is adsorbed on Pd clusters. On Pd-supported catalysts such as the 1.4% Pd/Al_2O_3 solid catalyst in this study, it can be considered that the L_1 species is formed on particles composed of one or two layers of Pd in interaction with the alumina support while the bridged CO species is formed on Pd tridimensional clusters and particles (with a heat of adsorption mainly independent of particle size). The L_2 species may involve low-coordinated atoms of these Pd particles. The discrepancy between the various studies on the particle size effect for values lower than 3 nm is probably related to the structure of the Pd particles. It can be supposed that this structure is a function of parameters such as the nature of the support and the preparation of the solid. The structure of the particles determines the ratio between the adsorbed species (L_1, L_2, B). The fact that sintering has no effect on the heats of adsorption of the adsorbed species can be interpreted by considering that: (a) the number of sites forming the L_1 species (Pd monolayer) decreases (decrease in intensity of IR band, Fig. 13) and yields new Pd particles, but without any modification of the metal/support interactions for the remaining sites; and (b) the number and orientation of the Pd particles are probably modified (change in B_1/B_2 ratio, Fig. 13) but without any effect on the heats of adsorption of the B species which are not strongly dependent on the exposed planes.

IV. CONCLUSIONS

An experimental procedure using (a) the change in the intensities of FTIR spectra of adsorbed CO species with adsorption temperature and (b) an adsorption model assuming a linear relationship between the heat of adsorption and coverage of the adsorbed species led to the following conclusions on the adsorption of CO on reduced 1.4% Pd/Al_2O_3:

A linear CO species, L_1, is formed with a heat of adsorption varying with coverage according to a linear relationship from 92 kJ/mol at $\theta = 0$ to 54 kJ/mol at $\theta = 1$.

Two bridged CO species, B_1 and B_2, are formed having similar heats of adsorption that vary with coverage according to a linear relationship from 168 kJ/mol at $\theta = 0$ to 92 kJ/mol at $\theta = 1$.

A second linear CO species, L_2, seems to be formed for which the heat of adsorption was not determined but is higher than 165 kJ/mol.

The heats of adsorption of the L_1, B_1, and B_2 species are modified neither by various pretreatments of the solid nor by sintering (aging) of the palladium particles.

The present results on the heats of adsorption of the L and B CO species concur well with the data on Pd-oriented planes, model Pd particles, and Pd-supported catalysts and reveal new aspects of the CO/Pd-supported particle system.

Some of the advantages of the present method of determination of the heats of adsorption using FTIR spectroscopy at high temperatures are: (a) the ease experimental procedure; (b) the use of conventional metal-supported catalysts; (c) the use of adsorption equilibrium conditions which avoids the difficulties encountered during a desorption procedure; and (d) the possibility of determining the heats of adsorption (at several coverages) of the various adsorbed species present simultaneously on the catalyst surface using a single isobar. The procedure described is a tool well adapted to study the effects of certain parameters, such as support, metallic dispersion, and bimetallic particles, on the heats of adsorption of CO on metal-supported catalysts. The difficulties concern the possible modifications of the metal surface during adsorption of CO at high temperatures.

ACKNOWLEDGMENTS

The authors acknowledge the E.C.I.A Company (Equipement et Composant pour l'Industrie Automobile), Bavans, France, which supported this work. Thanks are extended to Sylviane Bois for technical assistance.

REFERENCES

1. Choi, K. I., and Vannice, M. A., *J. Catal.* **127**, 465 (1991).
2. Valden, M., Keiski, R. L., Xiang, N., Pere, J., Aaltonen, J., Pessa, M., Maunula, T., Savimaki, A., Lahti, A., and Harkonen, M., *J. Catal.* **161**, 614 (1996).
3. Chesters, M. A., McDougall, G. S., Pemble, M. E., and Sheppard, N., *Surf. Sci.* **164**, 425 (1985).
4. Szanyi, J., Kuhn, W. K., and Goodman, D. W., *J. Vac. Sci. Technol. A* **11**, 1969 (1993).
5. Behm, R. J., Christmann, K., and Ertl, G., *J. Chem. Phys.* **73**, 2984 (1980).
6. Conrad, H., Ertl, G., Koch, J., and Latta, E. E., *Surf. Sci.* **43**, 462 (1974).
7. Dawies, P. W., and Lambert, R. M., *Surf. Sci.* **111**, L671 (1981).
8. Ramsier, R. D., Lee, K. W., and Yates, J. T., Jr., *Surf. Sci.* **327**, 243 (1995).
9. Chou, P., and Vannice, M. A., *J. Catal.* **104**, 17 (1987).
10. Kuhn, W. K., Szanyi, J., and Goodman, D. W., *Surf. Sci.* **274**, L611 (1992).
11. Kuhn, W. K., Szanyi, J., and Goodman, D. W., *Surf. Sci.* **303**, 377 (1994).
12. Pavlova, S. N., Sadykov, V. A., Razdodarov, V. A., and Paukshtis, E. A., *J. Catal.* **161**, 507 (1996).
13. Vannice, M. A., Wang, S. Y., and Moon, S. H., *J. Catal.* **71**, 152 (1981).
14. Sheu, L. L., Karpinski, Z., and Sachtler, W. M. H., *J. Phys. Chem.* **93**, 4890 (1989).
15. Liotta, L. F., Martin, G. A., and Deganello, G., *J. Catal.* **164**, 322 (1996).
16. Pitchon, V., Primet, M., and Pralliaud, H., *Appl. Catal.* **62**, 317 (1990).
17. Evans, J., Hayden, B. E., and Lu, G., *Surf. Sci.* **360**, 61 (1996).
18. Goyhenex, C., Croci, M., Claeys, C., and Henry, C. R., *Surf. Sci.* **352**, 475 (1996).
19. Hicks, R. F., Yen, Q. J., and Bell, A. T., *J. Catal.* **89**, 498 (1984).
20. Gorte, R. J., *J. Catal.* **75**, 164 (1982).
21. Demmin, R. A., and Gorte, R. J., *J. Catal.* **90**, 32 (1984).
22. Gravelle-Rumeau-Maillot, M., Pitchon, V., Martin, G. A., and Praliaud, H., *Appl. Catal.* **98**, 45 (1993).
23. Chafik, T., Dulaurent, O., Gass, J. L., and Bianchi, D., *J. Catal.* **179**, 503 (1998).
24. Voogt, E. H., Coulier, L., Gijzeman, O. L., and Geus, J. W., *J. Catal.* **169**, 359 (1997).
25. Van Hardeveld, R., and Hartog, F., *Adv. Catal.* **22**, 75 (1972).
26. Goetz, J., Volpe, M. A., Sica, A. M., Gigola, C. E., and Touroud, R., *J. Catal.* **167**, 314 (1997).
27. Bradshaw, A. M., and Hoffmann, F. M., *Surf. Sci.* **72**, 513 (1978).
28. Rieck, J. S., and Bell, A. T., *J. Catal.* **96**, 88 (1985).
29. Rieck, J. S., and Bell, A. T., *J. Catal.* **103**, 46 (1987).
30. Matolin, V., and Gillet, E., *Surf. Sci.* **238**, 75 (1990).
31. Stara, I., and Matolin, V., *Surf. Sci.* **313**, 99 (1994).
32. Rasband, P. B., and Hecker, W. C., *J. Catal.* **139**, 551 (1993).
33. Doyen, G., and Ert, G., *Surf. Sci.* **43**, 197 (1974).
34. Szanyi, J., and Goodmann, D. W., *J. Phys. Chem.* **98**, 2972 (1994).
35. Szanyi, J., Kuhn, W. K., and Goodmann, D. W., *J. Phys. Chem.* **98**, 2978 (1994).
36. Henry, C. R., Chapon, C., Goyhenex, C., and Monot, R., *Surf. Sci.* **272**, 283 (1994).
37. Ladas, S., Poppa, H., and Boudart, M., *Surf. Sci.* **102**, 151 (1981).
38. Stara, I., and Matolin, V., *Surf. Sci.* **313**, 99 (1994).
39. Cordatos, H., Bunluesin, T., and Gorte, R. J., *Surf. Sci.* **323**, 219 (1995).
40. Zilm, K. W., Bonneviot, L., Haller, G. L., Han, O. H., and Kermarec, M., *J. Phys. Chem.* **94**, 8495 (1990).
41. Sellidj, A., and Koel, B. E., *Surf. Sci.* **284**, 139 (1993).